IL NUOVO CIMENTO **38 C** (2015) 124
DOI 10.1393/ncc/i2015-15124-0

Colloquia: LaThuile15

Neutrino interactions on nuclei at MINERvA

M. F. Carneiro on behalf of the MINERvA Collaboration

CBPF - Centro Brasileiro de Pesquisas Físicas - Rua Dr. Xavier Sigaud 150, Urca, Rio de Janeiro, RJ, 22290-180, Brazil

received 2 October 2015

Summary. — Here we present analysis results from the MINERvA experiment for scattering of neutrinos on nucleus in an energy region of few GeV. These results cover a plethora of processes important for high precision neutrino oscillation measurements in which recent results have suggested that the currently used models are insufficient.

PACS 13.15.+g – Neutrino interactions.
PACS 25.80.Hp – Pion-induced reactions.
PACS 25.30.-c – Lepton-induced reactions.

1. – Description

The MINERvA experiment is a fully active, high resolution detector designed to study neutrino-nucleus scattering in the few-GeV region and provide inputs for neutrino oscillation experiments. The experiment also examines nuclear effects and parton distribution functions (PDFs) using a variety of targets materials. Precision neutrino measurements aiming to determine mass hierarchy, probe CP violation, or looking for new physics, require precise knowledge of cross sections, final states, and nuclear effects in neutrino scattering. These experiments need models that will correctly predict the rate of events for neutrino interactions, especially using medium-heavy materials such as steel, argon, carbon and oxygen. The true neutrino energy relation with the final state particles is also a key information for neutrino oscillation physics since the flavor oscillation probability depends on neutrino energy.

The detector is situated in Fermilab's NuMI beamline [1] along with the MINOS and NOvA experiments. During the period of 2010 through the Spring of 2012 the MINERvA detector took data in the "low energy" mode, in which the peak for the neutrino energy was around 3 GeV. Since then, the NuMI beamline is working in "medium energy" mode with the neutrino energy peak at 6 GeV.

MINERvA [2] is comprised of 120 hexagonal modules stacked along the beamline. The detector is segmented transversely into: the inner detector, with planes of solid scintillator and passive nuclear target regions of carbon, iron, lead and water; a region of pure scintillator strips; downstream electromagnetic calorimeter and hadronic calorimeters; and an outer detector composed of a frame of steel with embedded scintillator, which also serves as the supporting structure. The scintillator strips have a triangular shape that permits 3 mm of position resolution and are placed in adjacent planes offset by 60 degrees from each other, enabling a three-dimensional track reconstruction. The MINOS near detector [3] is situated two meters downstream of the MINERvA detector and serves as a magnetized muon spectrometer.

The calculation of cross section σ_i for N_j events in T interaction targets compared to B_j background predictions in bins of neutrino energy i and considering the detector efficiency of ϵ_i is given by

$$\sigma_i = \frac{U_{ij}(N_j - B_j)}{\Phi T \epsilon_i}, \tag{1a}$$

where Φ is the integrated neutrino flux in bin i and U_{ij} is an unfolding function that converts from reconstructed bins j to true bins i.

2. – Charged-current quasielastic scattering

Charged-current quasielastic (CCQE) scattering $\nu_l(\bar{\nu}_l) + n(p) \rightarrow l^-(l^+) + p(n)$ is the simplest process between a neutrino and a nucleon mediated by a W boson. We have good knowledge about neutrino-nucleon interactions from hydrogen and deuterium [4, 5] bubble chamber measurements. Neutrino event generators consider the nucleon to be quasi-free in a Relativistic Fermi Gas (RFG) [6] in order to correct for nuclear medium. Recent data, however, do not agree with the relativistic Fermi gas prediction motivating the MINERvA CCQE analysis presented here.

MINERvA's first CCQE results [7,8] select candidate events with vertex in the plastic scintillator portion of the detector, a muon in the final state with momentum and charge reconstructed in the MINOS near detector, and low hadronic recoil in the MINERvA detector to reduce deep inelastic scattering (DIS) and resonance backgrounds. Assuming that the scattering takes place in one single, at-rest, nucleon, we can use the muon (antimuon) to calculate Q^2 and produce a flux-integrated cross section $\mathrm{d}\sigma/\mathrm{d}Q^2$. Figure 1

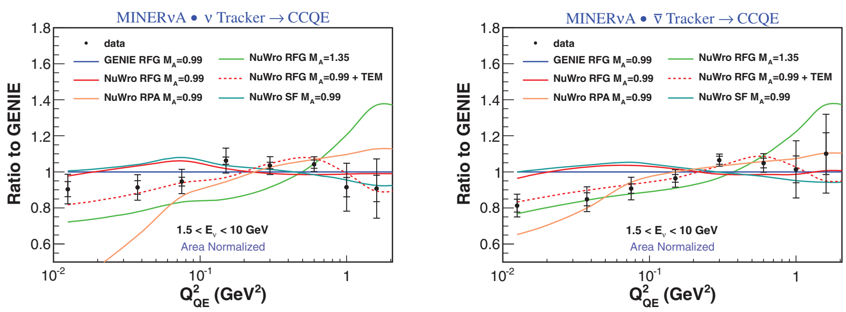

Fig. 1. – MINERvA ν_μ CCQE-like data shown as a function of Q^2 calculated from the muon kinematics as well as models from the NuWro generator [9] in a ratio to the GENIE event generator prediction. Neutrino data on the left and antineutrino on the right. In both cases the model predictions were weighted to the integral of the data producing a shape comparison where flux uncertainties largely cancel.

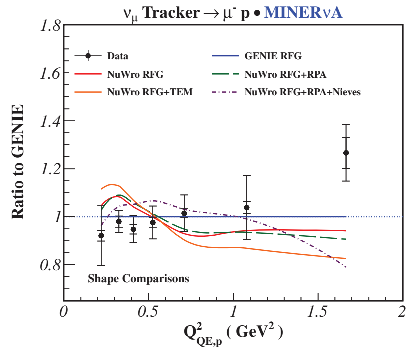

Fig. 2. – MINERvA ν_μ CCQE data shown as a function of Q^2 calculated from the proton kinematics as well as models from the NuWro generator in a ratio to the GENIE event generator prediction. The model predictions were weighted to the integral of the data producing a shape comparison were flux uncertainties largely cancel.

shows the results for antineutrino and neutrino analysis, with a number of model predictions. Each prediction has been scaled to match the integral of the data so we can have a shape comparison with reduced flux uncertainties, and then divided by the prediction of the GENIE generator [10]. As seen in other experimental results, the Fermi gas model from GENIE does not correctly predict the data. The better agreement comes from the prediction of the transverse enhancement model (TEM) [11], which includes parametrization of nucleon-nucleon correlations based on electron scattering data.

The second CCQE analysis [12] presented here uses a sample of events where not just the muon was identified, but also a proton. This analysis uses only the neutrino dataset and uses the proton kinematics to reconstruct Q^2. This excludes the need for the muon to enter the MINOS detector, for example, an event with a muon by exiting the side of MINERvA would be selected, which increase angular acceptance. As well as quasi-elastic events, this includes resonant or DIS events that undergo final-state interactions, leaving only nucleons in the final state. Quasi-elastics could produce more than one proton if the initial proton re-interacts in FSI and produces another, if we scatter from a correlated pair of nucleons. The result, shown in fig. 2 in the same format as fig. 1, shows a discrepancy with the GENIE prediction which is not reproduced by any of the models at high Q^2, demonstrating the need for improved modeling of the hadronic system in CCQE interactions.

3. – Charged-current single charged pion production

The delta resonance $\nu_\mu + p \to \mu^- + \Delta^{++} \to \mu^- + \pi^+ + p$ is the main process for pion production by neutrino scattering. Usually a resonance such as $\Delta(1232)$ is created and decays to a pion and nucleon. Final state interactions (FSI) can absorb the pion in interactions with nuclear targets, mimicking the quasi-elastic signal and making pion production a major background for detectors that use CCQE as their signal. On the other hand FSI can produce pions contaminating the quasi-elastic signal. The MINERvA pion production measurement [13] aims to examine the modeling of final state interactions by comparing distributions of pion kinematics to those predicted by models. The event selection applied the requirement for a muon that had reached the MINOS near detector,

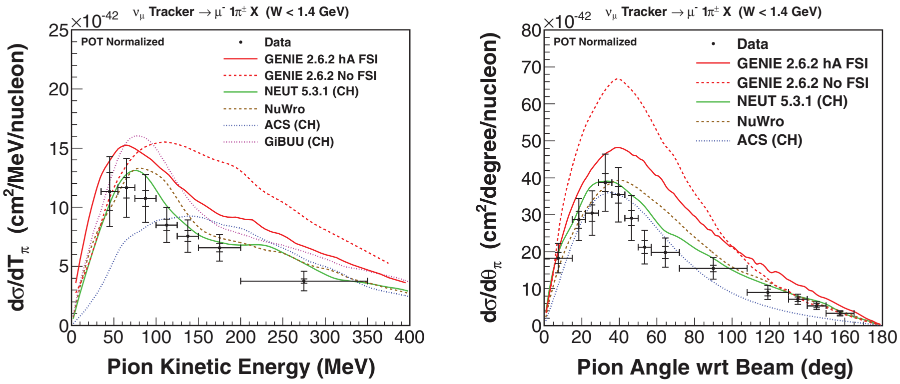

Fig. 3. – Flux-integrated differential cross section for muon neutrino events producing a single charged pion in MINERvA shown in function of pion energy and angle. Data is presented with several model predictions that were scaled to match the integral of the data.

and a candidate pion reconstructed inside the MINERvA detector without creating a hadron shower. Pions can be identified in MINERvA by their $\mathrm{d}E/\mathrm{d}x$ and the presence of a Michel electron from the pion to muon to electron decay chain. Figure 3 shows the resulting pion kinematics, after a data-driven background subtraction constrained by the $W > 1.4\,\mathrm{GeV}$ sideband along with several model predictions, including the GENIE event generator with and without the final state interactions implemented. The results show a strong preference for models that include a full treatment of FSI.

4. – Charged-current single neutral pion production by antineutrino

As in the last presented result, the delta resonance $\bar{\nu}_\mu + p \to \mu^+ + \Delta^0 \to \mu^+ + \pi^0 + n$ is the main process studied by this analysis. As the π^0 decays into two photons it can mimic an electron neutrino signal making this a important channel for oscillation experiments. This analysis [14] uses events with muons in the final state matched with MINOS data and antineutrino events that happened in the tracker region. Figure 4 shows the results for the pion kinematics and the data has a better agreement when final state interactions are included. This is the first measurement, at these energies, of the differential cross sections *vs.* π^0 kinematics for this pion production channel. These cross sections can be used as a benchmark to evaluate neutrino event generator performance for π^0 production by antineutrinos for current and future oscillation experiments.

5. – Charged-current scattering on different nuclei

The MINERvA detector upstream region has five passive targets of different materials as lead, iron and graphite, separated by between four and sixteen planes of scintillator. This configuration permits a study of the neutrino cross section dependence with nuclear mass. Also by looking into ratios of cross section measurements on each different passive material target to the same measurement in the tracker, which consists of CH scintillator, the flux uncertainty is largely canceled. These measurements [15] aim to address the necessity from oscillation experiments for accurate predictions for the neutrino cross section in specific materials as well as to investigate the EMC effect using neutrino-nucleus scattering.

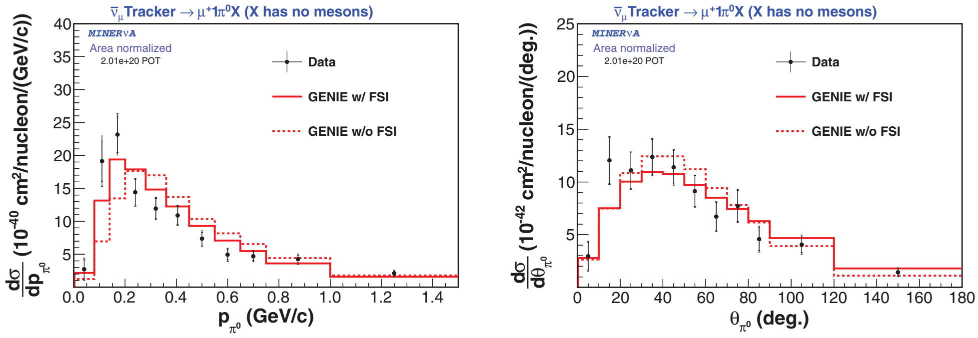

Fig. 4. – Flux-integrated differential cross section for antineutrino events producing a single neutral pion shown in function of pion energy and angle. MINERvA π^0 data is presented with GENIE event generator predictions with and without final state interaction implemented where both predictions were scaled to match the integral of the data.

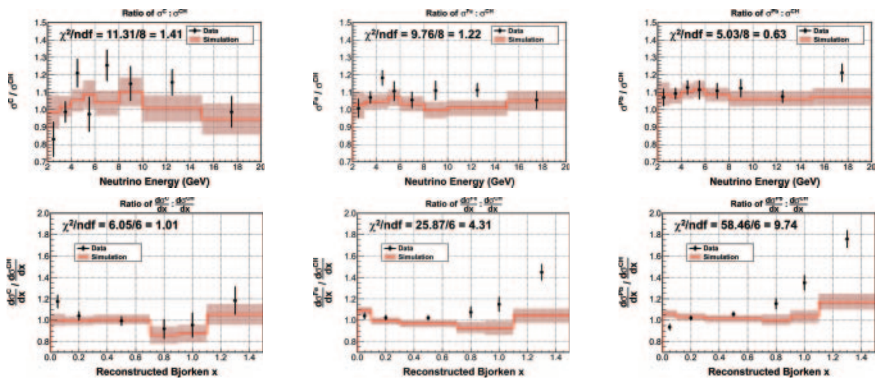

Fig. 5. – Ratios of charged current interaction cross sections on carbon, iron and lead to the cross section on plastic scintillator. The top row shows the ratio as a function of neutrino energy, while the bottom row shows the ratio as a function of Bjorken x.

We select neutrino events happening in the upstream part of the detector, inside the passive targets, and where the final state muon is matched to a muon event in MINOS. This last requirement constraints our angular acceptance to values less than 17 degrees with respect to the beam, and an energy above 2 GeV. Using a similar selection we can select events that happened in the tracker region and have results in the ratios between these two samples. Figure 5 shows this result as functions of E_ν and Bjorken x. The data are consistent with the prediction of GENIE in energy, but there's a discrepancy at high x, which increases with mass number of the nucleus. Around 60% of the events with values of $x > 0.7$ consist of CCQE events, so this is an important effect that needs to be understood by neutrino oscillation experiments.

6. – Conclusion

The MINERvA collaboration is looking into a large range of important neutrino-nucleus cross section measurements which aim to understand, test and improve the model of these processes, and thus to reduce systematics in oscillation experiments. The experiment is currently taking a new dataset in the Medium Energy beam configuration that will not only provide higher statistics for these analyses, but will also provide the ability to measure these processes on different nuclei.

* * *

This work was supported by the Fermi National Accelerator Laboratory under US Department of Energy contract No. DE-AC02-07CH11359 which included the MINERvA construction project. Construction support also was granted by the United States National Science Foundation under Award PHY-0619727 and by the University of Rochester. Support for participating scientists was provided by NSF and DOE (USA) by CAPES and CNPq (Brazil), by CoNaCyT (Mexico), by CONICYT (Chile), by CONCYTEC, DGI-PUCP and IDI/IGI-UNI (Peru), by Latin American Center for Physics (CLAF) and by RAS and the Russian Ministry of Education and Science (Russia). We thank the MINOS Collaboration for use of its near detector data. Finally, we thank the staff of Fermilab for support of the beamline and the detector.

REFERENCES

[1] Anderson K., Bernstein B., Boehnlein D., Bourkland K. R., Childress S. *et al.*, Fermilab-Design-1998-01 Technical Report (1998).

[2] The MINERvA Collaboration (Aliaga L. *et al.*), *Nucl. Instrum. Methods A*, **743** (2014) 130.

[3] MINOS Collaboration (Michael D. G. *et al.*), *Nucl. Instrum. Methods A*, **596** (2008) 190.

[4] Bodek A., Avvakumov S., Bradford R. and Budd H. S., *J. Phys.: Conf. Ser.*, **110** (2008) 082004.

[5] Kuzmin K. S., Lyubushkin V. V. and Naumov V. A., *Eur. Phys. J. C*, **54** (2008) 517.

[6] Smith R. and Moniz E., *Nucl. Phys. B*, **43** (1972) 605.

[7] The MINERvA Collaboration (Fiorentini G. A., Schmitz D. *et al.*), *Phys. Rev. Lett.*, **111** (2013) 022502.

[8] The MINERvA Collaboration (Fields L., Chvojka J. *et al.*), *Phys. Rev. Lett.*, **111** (2013) 022501.

[9] Graczyk K. M. and Sobczyk J. T., *Eur. Phys. J. C*, **31** (2003) 177.

[10] Andreopoulos C. *et al.*, *Nucl. Instrum. Methods A*, **288** (2010) 87.

[11] Bodek A., Budd H. and Christy M., *Eur. Phys. J. C*, **71** (2011) 1726.

[12] The MINERvA Collaboration (Walton T., Betancourt M. *et al.*), *Phys. Rev. D*, **91** (2015) 071301.

[13] The MINERvA Collaboration (Eberly B. *et al.*), arXiv:1406.6415 [hep-ex].

[14] The MINERvA Collaboration (Le T. *et al.*), arXiv:1503.02107 [hep-ex].

[15] The MINERvA Collaboration (Tice B. *et al.*), *Phys. Rev. Lett.*, **112** (2014) 231801.